AFRL-ML-WP-TR-1999-4015

SPLINE VARIATIONAL THEORY FOR COMPOSITE BOLTED JOINTS

E. IARVE

UNIVERSITY OF DAYTON RESEARCH INSTITUTE
300 COLLEGE PARK AVENUE
DAYTON, OH 45469-0168

JANUARY 1999

INTERIM REPORT FOR 09/15/1997 – 09/14/1998

MATERIALS AND MANUFACUTURING DIRECTORATE
AIR FORCE RESEARCH LABORATORY
AIR FORCE MATERIEL COMMAND
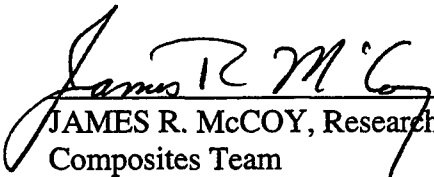WRIGHT-PATTERSON AIR FORCE BASE OH 45433-7734

DTIC QUALITY INSPECTED 4

19990820 070

NOTICE

Using Government drawings, specifications, or other data included in this document for any purpose other than Government procurement does not in any way obligate the U.S. Government. The fact that the Government formulated or supplied the drawings, specifications, or other data does not license the holder or any other person or corporation; or convey any rights or permission to manufacture, use, or sell any patented invention that may relate to them.

This report is releasable to the National Technical Information Service (NTIS). At NTIS, it will be available to the general public, including foreign nations.

This technical report has been reviewed and is approved for publication.

JAMES R. McCOY, Research Chemist
Composites Team
Structural Materials Branch

L. SCOTT THEIBERT, Chief
Structural Materials Branch
Nonmetallic Materials Division

ROGER D. GRISWOLD, Assistant Chief
Nonmetallic Materials Division
Materials and Manufacturing Directorate

REPORT DOCUMENTATION PAGE		*Form Approved* *OMB No. 0704-0188*

Public reporting burden for this collection of information is estimated to average 1 hour per response, including the time for reviewing instructions, searching existing data sources, gathering and maintaining the data needed, and completing and reviewing the collection of information. Send comments regarding this burden estimate or any other aspect of this collection of information, including suggestions for reducing this burden, to Washington Headquarters Services, Directorate for Information Operations and Reports, 1215 Jefferson Davis Highway, Suite 1204, Arlington, VA 22202-4302, and to the Office of Management and Budget, Paperwork Reduction Project (0704-0188), Washington, DC 20503.

1. AGENCY USE ONLY *(Leave blank)*	2. REPORT DATE JANUARY 1999	3. REPORT TYPE AND DATES COVERED INTERIM REPORT FOR 09/15/1997 - 09/14/1998	
4. TITLE AND SUBTITLE SPLINE VARIATIONAL THEORY FOR COMPOSITE BOLTED JOINTS			**5. FUNDING NUMBERS** C F33615-95-D-5029 PE 61102 PR 4347
6. AUTHOR(S) E. IARVE			TA 34 WU 10
7. PERFORMING ORGANIZATION NAME(S) AND ADDRESS(ES) UNIVERSITY OF DAYTON RESEARCH INSTITUTE 300 COLLEGE PARK AVENUE DAYTON, OH 45469-0168			**8. PERFORMING ORGANIZATION REPORT NUMBER** UDR-TR-1999-00001
9. SPONSORING/MONITORING AGENCY NAME(S) AND ADDRESS(ES) MATERIALS AND MANUFACTURING DIRECTORATE AIR FORCE RESEARCH LABORATORY AIR FORCE MATERIEL COMMAND WRIGHT-PATTERSON AFB, OH 45433-7734 POC: JAMES R. McCOY, AFRL/MLBC, 937-255-9063			**10. SPONSORING/MONITORING AGENCY REPORT NUMBER** AFRL-ML-WP-TR-1999-4015
11. SUPPLEMENTARY NOTES			
12a. DISTRIBUTION AVAILABILITY STATEMENT APPROVED FOR PUBLIC RELEASE, DISTRIBUTION UNLIMITED			**12b. DISTRIBUTION CODE**

13. ABSTRACT *(Maximum 200 words)*

The hybrid numerical approximation model for predicting stresses and strains in open-hole composites was refined. The model was also expanded to include singular full-field stress analysis of multi-interface composites under mechanical, thermal and bearing loads. The rigid fastener hole problem was also examined. This hybrid model, using spline variational theory and Reissner's variational principle, provides accurate solutions in the vicinity of the singularity. Convergence with coarse subdivisions was observed if the multiple singular terms of neighboring interfaces are included.

14. SUBJECT TERMS bolted joints, mechanics modeling, spline variational theory, open-hole composite, damage initiation			**15. NUMBER OF PAGES**
			16. PRICE CODE
17. SECURITY CLASSIFICATION OF REPORT Unclassified	**18. SECURITY CLASSIFICATION OF THIS PAGE** Unclassified	**19. SECURITY CLASSIFICATION OF ABSTRACT** Unclassified	**20. LIMITATION OF ABSTRACT** SAR

Standard Form 298 (Rev. 2-89) (EG)
Prescribed by ANSI Std. 239.18
Designed using Perform Pro, WHS/DIOR, Oct 94

CONTENTS

FIGURES

FIGURES (Concluded)

FOREWORD

This report was prepared by the University of Dayton Research Institute under Air Force Contract No. F33615-95-D-5029, Delivery Order No. 0004. The work was administered under the direction of the Nonmetallic Materials Division, Materials and Manufacturing Directorate, Air Force Research Laboratory, Air Force Materiel Command, with Dr. James R. McCoy (AFRL/MLBC) as Project Engineer.

This report was submitted in January 1999 and covers work conducted from 15 September 1997 through 14 September 1998.

EXECUTIVE SUMMARY

Stress analysis of composite laminates with open and filled holes is an important issue due to the broad range of composite bolted joining applications. The inherent difficulty of the three-dimensional analysis of these structures is due to singular stress behavior near the laminate edge and ply interfaces. Numerical stress analysis methods such as commercial FEM are known to produce mesh sensitive results and boundary condition errors in these regions. This report reflects further development of the combined analytical asymptotic solutions and B-spline-based numerical approximation to overcome these difficulties. The method of superposition of a hybrid and displacement approximation, developed in a previous report and demonstrated for simple laminates with open holes, is extended for singular full-field stress analysis in multi-interface practical composites under mechanical, thermal and bearing loading. The displacement approximation is based on polynomial B-spline functions. This method provides determination of the coefficient of the singular term along with convergent stress components including the singular regions. Reissner's variational principle was employed. Uniaxial loading and residual stress calculation were considered for a quasi-isotropic IM7/5250 $[45/90/-45/0]_s$ laminate. A convergence study showed that accurate values of the coefficient of the singular term of the asymptotic stress expansion could be obtained with coarse out-of-plane and in-plane subdivisions. The interaction between singular terms on neighboring interfaces was found to be important for convergence with coarse subdivisions. Converged transverse interlaminar stress components as a function of distance from the hole edge were shown for all examples. The hybrid approximation developed for the open-hole problems was extended to rigid fastener hole problems. A near-singular term of the asymptotic expansion, present in the filled-hole

problem only, was taken into account in order to obtain a convergent solution with a coarse spline approximation mesh. A bearing-loaded $[45/-45]_s$ laminate was considered, and the multiplicative factors of the singular stress terms at the hole edge and ply interface were obtained .

1. INTRODUCTION

A hybrid approximation model was proposed in *[1,2]* for singular full-field stress calculation in laminates with open holes. The model was developed for single interface laminates under mechanical loading. In the present report this model is extended for stress analysis in practical laminates with multiple interfaces under thermal and/or mechanical loading. Another extension reported below considers rigid fastener hole laminates loaded in bearings.

The model developed is based on Reissner's variational principle and is intended to reflect the singularities which arise at each interface at the boundary of the hole. Hybrid approximation functions to be developed have the following characteristics:

(1) They include the asymptotic solution, thus representing the directional nonuniqueness of the solution. It is only in this manner that one can embed the proper singular field. The fact that the asymptotic solution results from the three-dimensional problem by truncating the spatial derivatives in the circumferential direction *[3]* will be used to construct hybrid stress functions.

(2) Two independent (B-spline) displacement functions are considered. One is related to the regular and the other to the singular portion of the stress field. It is undesirable to use the asymptotic displacement functions in the displacement approximation, since the calculation of their derivatives in the circumferential direction, required in the variational formulation, is only possible numerically. It is assumed that the displacements related to the singular stresses will also be approximated with splines. Thus the approximations of stresses and displacements are made independently.

2. PROBLEM STATEMENT

Consider a rectangular N-layer laminate built of orthotropic layers with length L in the x-direction, width A in the y-direction, and thickness H. Individual ply thicknesses are $h_p = z^{(p)} - z^{(p-1)}$, where $z = z^{(p)}$ and $z = z^{(p-1)}$ are upper and lower surfaces of the p-th ply, respectively. The origin of the x,y,z coordinate system is in the lower left corner of the plate, as shown in Figure 1. A circular opening of diameter D with the center at $x = x_c$ and $y = y_c$ is considered. Uniaxial loading is applied via displacement boundary conditions at the lateral sides (x=0,L):

$$- u_x(0, y, z) = u_x(L, y, z) = u_0,$$
$$u_y(0, y, z) = u_y(L, y, z) = 0, \tag{1}$$

The transverse displacement is not constrained aside from a rigid body constant, and the respective traction $T_z = 0$ is prescribed. The edge of the opening is part of the traction prescribed loading boundary S_T, so that

$$\sigma_{ij} n_j = T_i(x_i), x_i \in S_T,$$

or mixed boundary conditions in the case of the rigid fastener

$$u_r = 0, \sigma_{ij} n_j = T_i(x_i), i \neq r, x_i \in S_T$$

where tractions T_i are known. Indices $i,j=1,2,3$ correspond to directions x,y,z, or r,θ,z, respectively. The lateral edges $y=0,A$ and the surfaces $z=0,H$ also belong to S_T. The constitutive relations in each ply are as follows:

$$\sigma_{ij} = C_{ijkl}^p (\varepsilon_{kl} - \alpha_{kl}^p \Delta T)$$

where C_{ijkl}^p and α_{kl}^p are elastic moduli and thermal expansion coefficients of the p-th orthotropic ply, and ΔT is the temperature change. A cylindrical coordinate system r, θ, z with the origin at $(x_c, y_c, 0)$ is introduced.

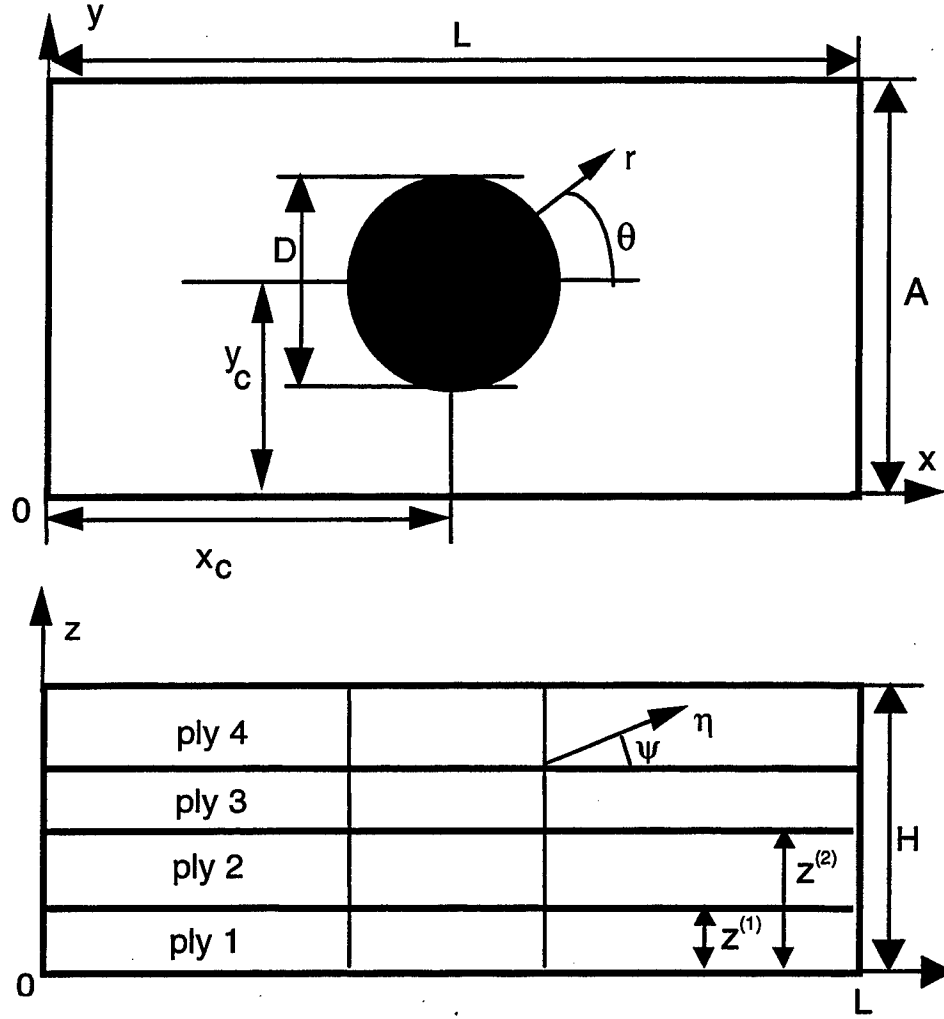**Figure 1. Plate with the Filled Hole and Coordinate Systems.**

$$x = r\cos\theta + x_c, y = r\sin\theta + y_c, z = z.$$

According to the asymptotic analysis performed in earlier papers *[3,4]*, the stresses in the vicinity of the hole edge and the interface between the *p* and *p+1* plies are thought to be of the form:

$$\sigma_{ij} = \sum_{\lambda} K_s(\theta)\eta^{\lambda-1} f_{ij}(\psi,\theta) + bounded\ function.$$

The first terms represent the unbounded ($0<\mathrm{Re}(\lambda)<1$) singular stress terms, where η and ψ are local coordinates introduced in the cross section $\theta=\mathrm{const}$ (Figure 1.b) according to equation

$$\eta\cos\psi = r - D/2, \quad \eta\sin\psi = z - z^{(p)}. \tag{2}$$

The asymptotic solution is normalized similar to [4] so that

$$K_p(\theta) = \lim_{\eta\to o}[\eta^{1-\lambda}\sigma_{zz}(D/2+\eta\cos\psi, z^{(p)}, \theta)].$$

The singular term

$$a_{ij} = \eta^{\lambda-1}f_{ij}(\psi,\theta)$$

is a solution of the asymptotically derived two-dimensional problem and satisfies neither the three-dimensional equilibrium nor compatibility equations in any finite volume around the curved boundary. However it does satisfy the traction-free boundary conditions on the hole edge as well as the interface continuity conditions in the limit $\eta\to0$. We shall consider one singular term at each angular location at each interface at the open-hole edge, with the extension to an arbitrary number of terms at the same singular point being straightforward. The displacement components and bounded portion of the stresses will be approximated by using cubic spline functions, and Reissner's variational principle will be applied in order to obtain $K_p(\theta)$ and the unknown spline approximation coefficients. The asymptotic solution near the orthotropic ply interface and the hole edge will be considered next.

3. ASYMPTOTIC SOLUTION

Consider a region around the hole edge and the interface between plies p and p+1. A local coordinate system η, ψ is introduced in the radial cross section θ=const according to equation (2). In this coordinate system $0 \leq \psi \leq \dfrac{\pi}{2}$ in the upper ply and $-\dfrac{\pi}{2} \leq \psi \leq 0$ in the lower one. For an arbitrary function F:

$$\frac{\partial F}{\partial r} = \Lambda_t F, \qquad \frac{\partial F}{\partial z} = \Lambda_n F,$$

where

$$\Lambda_t F = \frac{\partial F}{\partial \eta}\cos\psi - \frac{1}{\eta}\frac{\partial F}{\partial \psi}\sin\psi, \quad \Lambda_n F = \frac{\partial F}{\partial \eta}\sin\psi + \frac{1}{\eta}\frac{\partial F}{\partial \psi}\cos\psi.$$

In Cartesian coordinates the derivatives can be calculated as

$$\begin{aligned}
\frac{\partial F}{\partial x} &= (\cos\theta)\Lambda_t F - \frac{\sin\theta}{D/2+\eta\cos\psi}\frac{\partial F}{\partial \theta}, \\
\frac{\partial F}{\partial y} &= (\sin\theta)\Lambda_t F + \frac{\cos\theta}{D/2+\eta\cos\psi}\frac{\partial F}{\partial \theta}.
\end{aligned} \tag{3}$$

If $\eta \rightarrow 0$, then the first terms in the right-hand side of both equations (3) are of the order F/η, and the second terms are of order F. Thus for small η the expressions for derivatives (3) are truncated by retaining only the first terms, so that:

$$\frac{\partial F}{\partial x} \cong \left(\frac{\partial F}{\partial x}\right)_\theta = \frac{\partial F}{\partial r}\cos\theta = \Lambda_t F \cos\theta,$$

$$\frac{\partial F}{\partial y} \cong \left(\frac{\partial F}{\partial y}\right)_\theta = \frac{\partial F}{\partial r}\sin\theta = \Lambda_t F \sin\theta, \qquad \eta \to 0 \qquad (4)$$

$$\left(\frac{\partial F}{\partial z}\right)_\theta = \frac{\partial F}{\partial z} = \Lambda_n F$$

where the notation $(\ )_\theta$ implies truncation by deletion of the θ derivative. Although these equations are exact in the limit $\eta \to 0$ only, we shall use these derivatives through a finite volume to construct the hybrid approximation. Under these assumptions the Navier equations of a given ply will simplify to:

$$(\mathbf{A}\Lambda_t\Lambda_t + \mathbf{B}\Lambda_n\Lambda_t + \mathbf{C}\Lambda_n\Lambda_n)\begin{bmatrix} u_x \\ u_y \\ u_z \end{bmatrix} = 0,$$

where the 3 x 3 matrices $\mathbf{A}, \mathbf{B}, \mathbf{C}$ are given in the Appendix and depend upon the elastic moduli and θ. Note that the thermal expansion coefficients do not enter these equations due to the assumption of uniform temperature change. The solution of the Navier equations can be found in the form

$$u_i = \sum_\lambda v_i^p(\eta^\lambda, \psi, \theta) + U_i^p(\eta, \psi, \theta)$$

where $U_i^p(\eta, \psi, \theta)$ is a particular solution and $\sum_\lambda v_i^p(\eta^\lambda, \psi, \theta)$ is the homogeneous solution. Nonhomogeneous boundary conditions resulting from nonzero prescribed tractions or thermal mismatch can be satisfied with a piecewise polynomial particular solution of appropriate order, provided that the prescribed tractions are smooth and bounded within the ply though perhaps discontinuous at the interfaces. The thermal expansion strains are not present for the homogeneous solution and will be determined in a particular solution. We

shall be interested in the homogeneous solutions v_i^p, which have essentially nonpolynomial format, and the respective tractions satisfying homogeneous boundary conditions. The homogeneous solution of the displacement field can be written as [3]:

$$v_i^p = \eta^\lambda \sum_{k=1}^{6} \gamma_k d_{ki}^p (\sin\psi + \mu_k^p \cos\psi)^\lambda ,$$

where the superscript p refers to the ply number. It will be understood that coefficients μ_k and vectors $\{ d_{ki} \}$ are constants for each ply; therefore the superscript is subsequently omitted, unless needed for clarity. The stresses from the homogeneous solution are

$$\sigma_{ij}^p = C_{ijkl}^p \left(\left(\frac{\partial v_k^p}{\partial x_l} \right)_\theta + \left(\frac{\partial v_l^p}{\partial x_k} \right)_\theta \right),$$

where the truncated derivatives are calculated by using expressions (4). The expression for the stresses may be written in the form

$$\sigma_{ij}^p = \lambda \eta^{\lambda-1} \sum_{k=1}^{6} \gamma_k c_{ij}^{k,p} (\sin\psi + \mu_k \cos\psi)^{\lambda-1} ,$$

Coefficients $c_{ij}^{k,p}$, defined in [3], depend upon elastic moduli of the p-th ply. It was taken into account that the following relationship applies for the differential operators

$$\Lambda_t v_i^p = \lambda \eta^{\lambda-1} \sum_{k=1}^{6} \gamma_k d_{ki} \mu_k (\sin\psi + \mu_k \cos\psi)^{\lambda-1} ,$$

$$\Lambda_n v_i^p = \lambda \eta^{\lambda-1} \sum_{k=1}^{6} \gamma_k d_{ki} (\sin\psi + \mu_k \cos\psi)^{\lambda-1} ,$$

which leads to the following characteristic equation for obtaining μ_k:

$$\det[\mathbf{A}\mu_k^2 + \mathbf{B}\mu_k + \mathbf{C}] = 0 ,$$

where $\{ d_{ki} \}$ are eigenvectors of the characteristic matrix:

$$[\mathbf{A}\mu_k^2 + \mathbf{B}\mu_k + \mathbf{C}]\begin{bmatrix} d_{k1} \\ d_{k2} \\ d_{k3} \end{bmatrix} = 0.$$

The power λ and coefficients γ_k are defined from the boundary conditions of displacement and traction continuity at the interface between plies p and p+1

$$\psi = 0: \ v_i^p(\eta, 0, \theta) = v_i^{p+1}(\eta, 0, \theta), \ \sigma_{zi}^p(\eta, 0, \theta) = \sigma_{zi}^{p+1}(\eta, 0, \theta), \ i = x, y, z,$$

and the traction-free open-hole boundary conditions:

$$\sigma_{ri}^{p+1}(\eta, \frac{\pi}{2}, \theta) = 0, \ i = r, \theta, z,$$

$$\sigma_{ri}^p(\eta, -\frac{\pi}{2}, \theta) = 0, \ i = r, \theta, z,$$

or the rigid fastener frictionless contact conditions:

$$u_r^{p+1}(\eta, \frac{\pi}{2}, \theta) = \sigma_{ri}^{p+1}(\eta, \frac{\pi}{2}, \theta) = 0, \ i = \theta, z,$$

$$u_r^p(\eta, -\frac{\pi}{2}, \theta) = \sigma_{ri}^p(\eta, -\frac{\pi}{2}, \theta) = 0, \ i = \theta, z.$$

Nontrivial solutions of the homogeneous boundary value problem exist for discrete values of λ only. Coefficients γ_k are obtained to satisfy the interfacial and hole edge boundary conditions. We shall be interested in the solutions when $0 < \text{Re}(\lambda) < 1$. These terms provide unbounded stresses which dominate the solution for small η. In the context of the present work, laminates with more than one interface will be considered, and the singular asymptotic terms will be used at each interface. For convenience, we will introduce an analytical continuation of the asymptotic displacements into all plies of the laminate. Thus we extend the definition of the displacement vector v_i^p and stress components a_{ij}^p for the

asymptotic solution associated with interface $z^{(p)}$ between plies p and p+1 depending upon the properties of the ply in which ψ is located[1]

$$v_i^p = \begin{cases} \eta^\lambda \sum\limits_{k=1}^{6} \gamma_k d_{ki}^{p+1} (\sin\psi + \mu_k^{p+1} \cos\psi)^\lambda , \psi > 0 \\ \eta^\lambda \sum\limits_{k=1}^{6} \gamma_k d_{ki}^{p} (\sin\psi + \mu_k^{p} \cos\psi)^\lambda , \psi \le 0 \end{cases}, \qquad (5)$$

and

$$a_{ij}^p = \begin{cases} \lambda\eta^{\lambda-1} \sum\limits_{k=1}^{6} \gamma_k c_{ji}^{k,q} (\sin\psi + \mu_k^{p+1} \cos\psi)^{\lambda-1} , \psi > 0, q = p+1,...,N \\ \lambda\eta^{\lambda-1} \sum\limits_{k=1}^{6} \gamma_k c_{ji}^{k,q} (\sin\psi + \mu_k^{p} \cos\psi)^{\lambda-1} , \psi \le 0, q = 1,...,p \end{cases} , z^{(q-1)} \le \eta\sin\psi + z^{(p)} < z^{(q)}$$

$$(6)$$

These functions are defined through the entire laminate thickness. The stresses a_{ij}^p are calculated from strains defined by the truncated derivatives of displacements v_i^p using the elastic moduli of that ply where the stresses are evaluated. The asymptotic solution obtained between plies p and p+1 will provide a nonzero stress contribution in a large area surrounding the singular point due to the weak character of singularity $\lambda-1\sim-0.05$ (references *[1-4]*) between similar orthotropic layers with different fiber orientations for the open hole.

---

[1] Note that we have refrained from using indices on the variables η an ψ since they always emanate from the singular point at $z=z^{(p)}$. Also λ has been given no subscript as we only use the lowest possible value at $z=z^{(p)}$.

11

4. VARIATIONAL FORMULATION

Displacement components are represented as

$$u_i = u_i^s + u_i^r,$$ (7)

where the displacements u_i satisfy boundary conditions (1). The term u_i^s is associated with singular stress components and the second term u_i^r with bounded stress components. The stresses will be assumed as

$$\sigma_{ij} = \sigma_{ij}^{hyb} + \sigma_{ij}^r,$$ (8)

The stresses σ_{ij}^{hyb} and displacements u_i^s are independently assumed. The stresses σ_{ij}^r and displacements u_i^r are related as follows

$$\sigma_{ij}^r = C_{ijkl}^q (u_{(k,l)}^r - \alpha_{klj}^q \Delta T),$$ (9)

where C_{ijkl}^q and α_{kl}^q are elastic moduli and thermal expansion coefficients of the q-th orthotropic ply, ΔT is the temperature change, and

$$u_{(i,j)} = \frac{1}{2}\left(\frac{\partial u_i}{\partial x_j} + \frac{\partial u_j}{\partial x_i}\right).$$ (10)

Reissner's variational principle $\delta R = 0$ is employed, where the functional R is given by equation

$$R = \iiint_V \left(-\Phi(\sigma_{ij}, \Delta T) + \sigma_{ij} u_{(i,j)}\right) dV - \iint_{S_T} T_i u_i ds.$$ (11)

and

$$\Phi(\sigma_{ij}, \Delta T) = \frac{1}{2} S_{ijkl}^q \sigma_{ij} \sigma_{kl} + \sigma_{ij} \alpha_{ij}^q \Delta T, \{S_{ijkl}^q\} = \{C_{ijkl}^q\}^{-1}$$

12

The surface tractions T_i in equation (11) are considered in a generalized sense, meaning that on the portion of the surface S_t, not belonging to the contact surface between the fastener and the hole, they are prescribed. On the contact surface these tractions are unknown, and T_i denotes the Lagrangian multiplier introduced to apply the boundary condition $u_r=0$. Substituting equations (7) and (8) into (11), one obtains after algebraic manipulations and use of Betti's law:

$$R = \iiint\limits_V \left[-\Phi(\sigma_{ij}^{hyb}, 0) + \sigma_{ij}^{hyb} u_{(i,j)}^s - W(u_{(i,j)}^s, 0) \right] dV \\ + \iiint\limits_V W(u_{(i,j)}^r + u_{(i,j)}^s, \Delta T) dV - \iint\limits_{S_T} T_i (u_i^r + u_i^s) ds. \tag{12}$$

where

$$W(\varepsilon_{ij}, \Delta T) = \frac{1}{2} C_{ijkl}^q (\varepsilon_{ij} - \alpha_{ij}^q \Delta T)(\varepsilon_{kl} - \alpha_{kl}^q \Delta T)$$

The goal of the formulation is to treat problems when the external tractions T_i and/or the interfacial tractions cannot be approximated pointwise by using the same shape functions as the displacement components or their derivatives. Let the functions X_m be the basis functions for approximation of the displacements u_i^r, and the functions Y_m – those for the displacements u_i^s. Then the following systems of equations will be obtained by taking the variations with respect to the unknown approximation coefficients

$$\iiint\limits_V \left[C_{ijkl}^q (u_{(k,l)}^r - \alpha_{kl}^q \Delta T) + C_{ijkl}^q u_{(k,l)}^s \right] X_{m,j} dV = \iint\limits_{S_T} T_i X_m dS$$

$$\iiint\limits_V \left[C_{ijkl}^q (u_{(k,l)}^r - \alpha_{kl}^q \Delta T) + \sigma_{ij}^{hyb} \right] Y_{m,j} dV = \iint\limits_{S_T} T_i Y_m dS$$

Both sets of basis functions X_m and Y_m in the present context are of the same piecewise polynomial nature. Without restricting the generality, one might assume that they are the

same. Indeed, one might always redefine the systems of basis functions $\{X_m\}$ and $\{Y_m\}$ as $\{X_m\} \cup \{Y_m\}$. In this case the equations can be rewritten as:

$$\iiint_V \left[C_{ijkl}^q (u_{(k,l)}^r + u_{(k,l)}^s - \Delta T \alpha_{kl}^q) \right] X_{m,j} dV = \iint_{S_T} T_i X_m dS \tag{13a}$$

$$\iiint_V \left[C_{ijkl}^q u_{(k,l)}^s \right] X_{m,j} dV = \iiint_V \sigma_{ij}^{hyb} X_{m,j} dV \tag{13b}$$

Integrating by parts and adding the equations to each other, one obtains

$$\iiint_V \left[C_{ijkl}^q u_{(k,l),j}^r + \sigma_{ij,j}^{hyb} \right] X_m dV + \iint_{S_T} [T_i - (C_{ijkl}^q (u_{(k,l)}^r - \Delta T \alpha_{ij}^q) + \sigma_{ij}^{hyb}) n_j] X_m dS = 0$$

The first term of the above equation contains the weak form of the equilibrium equations and the second term – the weak form of the boundary conditions. They are interconnected, meaning that if the boundary conditions are not satisfied in the weak form,[2] then the error in the equilibrium equations will not vanish even in the weak form, i.e. it will not be orthogonal to each of the displacement approximation basis functions. In the next section a form of σ_{ij}^{hyb} will be proposed so that the boundary conditions on the hole edge and the interfacial continuity conditions will be satisfied. In this case, provided that equations (13a,b) are also satisfied, the stresses (8) will satisfy the equilibrium equations in the weak sense, even in the vicinity of the singularities.

---

[2] The error is orthogonal to each of the displacement approximation basis functions.

5. HYBRID APPROXIMATION

Consider the exact stresses associated with the displacement u_i^s in the q-th ply:

$$\sigma_{ij}^s = C_{ijkl}^q u_{(k,l)}^s$$

The thermal expansion term is not included with the singular displacement portion, since it was accounted for in (9). The stresses resulting from displacement field u_i^s are modified to include the singular asymptotic stress field (6). We shall calculate the strain field generated by the truncated derivatives of the displacements, as follows

$$2u_{(i,j)_\theta}^s = \left(\frac{\partial u_i^s}{\partial x_j}\right)_\theta + \left(\frac{\partial u_j^s}{\partial x_i}\right)_\theta,$$

where $\left(\dfrac{\partial u_i^s}{\partial x_j}\right)_\theta$ are calculated according to truncated expressions (4). The contribution of the stresses generated by these strains is given by the asymptotic stress field (6), so that the hybrid stresses associated with displacements u_i^s are

$$\sigma_{ij}^{hyb} = \sigma_{ij}^s + \sum_{p=1}^{N-1} K_p(\theta)a_{ij}^p - s_{ij}$$

where

$$s_{ij} = C_{ijkl}^q u_{(k,l)_\theta}^s . \tag{14}$$

The unknown functions of the hybrid approximation (7) and (8) are the displacements u_i^s, u_i^r and coefficients K_p. Practically speaking, we expect the hybrid approximation to be needed only in the vicinity of the hole edge. Let the volume Γ be bounded by the hole edge, the top and bottom surfaces and $r=r_0$: $D/2<r_0<\min(L,A)$. Inside this region stresses are given by

equations (8), and outside this region $u_i^s = 0$ and $\sigma_{ij} = \sigma_{ij}^r$. The total displacement must be

continuous at the internal boundary $r=r_0$. It can be satisfied easily if the unknown

displacement approximation functions are the total displacement u_i and u_i^s instead of u_i^r and

u_i^s. The stress approximation (8) can be rewritten accordingly:

$$\sigma_{ij} = \sigma_{ij}^u + \sum_{p=1}^{N-1} K_p(\theta) a_{ij}^p - s_{ij} \qquad (15)$$

where

$$\sigma_{ij}^u = C_{ijkl}^q (u_{(k,l)} - \alpha_{kl}^q \Delta T). \qquad (16)$$

6. GOVERNING EQUATIONS

Taking into account equations (15) and the change to independent displacement

functions u_i and u_i^s, equations (13) will attain the following form

$$\iiint\limits_{V} \left[C_{ijkl}^q (u_{(k,l)} - \Delta T \alpha_{kl}^q) \right] X_{m,j} dV = \iint\limits_{S_T} T_i X_m dS \qquad (17)$$

$$\iiint\limits_{\Gamma} \left[C_{ijkl}^q u_{(k,l)_\theta}^s \right] X_{m,j|\theta} dV = \iiint\limits_{\Gamma} \sum_{p=1}^{N-1} K_p(\theta) a_{ij}^p X_{m,j|\theta} dV \qquad (18)$$

where $X_{m,j|\theta}$ are based on truncated derivatives (4). Equation (17) follows from (13a) after

substituting (7) and allows one to calculate the total displacement in an independent problem

under the given traction and displacement boundary conditions (1). Several steps have been

undertaken to reduce (13b) to (18). It has been considered that the hybrid approximation is

defined inside Γ only and that truncated derivatives (4) were used in the hybrid stress

approximation. The spatial derivatives appearing in (18) are also truncated derivatives,

meaning that auxiliary problem (18) is a two-dimensional problem with the θ-coordinate as a

parameter. A substitution

$$u_i^s = \sum_{p=1}^{N-1} K_p u_i^{s,p}$$

provides a solution of equation (18) for arbitrary K_p if

$$\iiint\limits_{\Gamma} \left[C_{ijkl}^q u_{(k,l)_\theta}^{s,p} \right] X_{m,j|\theta} dV = \iiint\limits_{\Gamma} a_{ij}^p X_{m,j|\theta} dV, \; p=1,\ldots,N-1, \qquad (19)$$

The displacement boundary conditions on the singular components $u_i^{s,p}$ must exclude rigid

body motion and be consistent with (5), i.e. no surface displacements can be prescribed for

$u_i^{s,p}$ on $S_T \cap \partial\Gamma$. Equation (19) provides the weak form of the equality of tractions $a_{ij}^p n_j$

and $C_{ijkl}^q u_{(k,l)_\theta}^{s,p} n_j$ on the portion of $\partial\Gamma$ inside the laminate (r=r$_0$), provided that no surface

17

displacements are prescribed for $u_i^{s,p}$ there. If the distance between this boundary and the hole edge is chosen sufficiently large, then the resulting traction discontinuity at this boundary for the stress field (15) may be reduced arbitrarily by increasing the numerical subdivision for the auxiliary problem. The following boundary conditions, consistent with (5), were imposed

$$u_r^{s,p}(D/2, z^{(p)}, \theta) = u_\theta^{s,p}(D/2, z^{(p)}, \theta) = 0, \quad u_z^{s,p}(r_0, z^{(p)}, \theta) = 0, \tag{20}$$

The stress approximation after the substitution can be rewritten as

$$\sigma_{ij} = \sigma_{ij}^u + \sum_{p=1}^{N-1} K_p(\theta)(a_{ij}^p - s_{ij}^p) \tag{21}$$

where

$$s_{ij}^p = C_{ijkl}^q u_{(i,j)_\theta}^{s,p}$$

18

7. DETERMINATION OF $K_p(\theta)$

The error in boundary conditions near the singularity from (17) is a result of approximating the directionally nonunique singular stress field by polynomials. The directional nonuniqueness means that for $\eta \to 0$, the stresses a_{ij}^p may tend to plus or minus infinity depending upon ψ. The polynomial approximation provides unique and finite stress values at every point of a given ply. The values of the stress intensity factors are obtained to enforce single-valuedness of the nonsingular portion $\sigma_{ij}^u - K_p(\theta)s_{ij}^p + \sum_{\substack{q=1, \\ q \ne p}}^{N-1} K_q(\theta)(a_{ij}^q - s_{ij}^q)$ at the singular point. Consider the interface $z=z^{(p)}$ between the p and the $p+1$-st ply. Let $P_i^{(p)}(\eta)$ be the interlaminar traction on the interface $z=z^{(p)}$ in the vicinity of the edge ($P_i^{(p)}(0)=\pm\infty$). Then, at the hole edge six traction boundary conditions have to be simultaneously satisfied

$$T_i = \sigma_{ij}n_j^h, P_i^{(p)}(\eta) = \sigma_{ij}n_j^p,$$

Thus one stress component, namely σ_{rz}, will appear in two equations which are

$$T_z = \sigma_{rz}(\eta,\pm\frac{\pi}{2},\theta), P_r^{(p)}(\eta) = \sigma_{rz}(\eta,0,\theta)$$

These equations can only be satisfied if

$$\lim_{\eta \to 0}[T_z - K_p(\theta)a_{rz}^p(\eta,\frac{\pi}{2},\theta)] = \lim_{\eta \to 0}[P_r - K_p(\theta)a_{rz}^p(\eta,0,\theta)] =$$
$$= \sigma_{rz}^u(\frac{D}{2},z^{(p)},\theta) - K_p(\theta)s_{ij}^p(\frac{D}{2},z^{(p)},\theta) + \sum_{\substack{q=1, \\ q \ne p}}^{N-1} K_q(\theta)[a_{ij}^q(\frac{D}{2},z^{(p)},\theta) - s_{ij}^q(\frac{D}{2},z^{(p)},\theta)] \tag{22}$$

These equations are necessary conditions to make the polynomial part of the stress tensor single-valued. It is worth noting that if instead of a corner one has a crack, i.e. $n_i^h = -n_i^p$,

then we shall have three pairs of single-valuedness conditions, one per each stress component in the plane normal to the crack. It will require three stress intensity factors: Mode I, II and III. In the case of a hole edge, we have only one interlaminar stress component which requires the single-valuedness condition: σ_{rz}. The criterion for determining $K_p(\theta)$ will be the continuity of the nonsingular part of σ_{rz} stress component at the singular points, i.e.

$$
\begin{aligned}
\Delta\left[\sigma_{ij}^u(\frac{D}{2}, z^{(p)}, \theta)\right] = K_p(\theta)\Delta\left[s_{ij}^p(\frac{D}{2}, z^{(p)}, \theta)\right] + \\
+ \sum_{\substack{q=1, \\ q \neq p}}^{N-1} K_q(\theta)\Delta\left[a_{ij}^q(\frac{D}{2}, z^{(p)}, \theta) - s_{ij}^q(\frac{D}{2}, z^{(p)}, \theta)\right], \quad p = 1,...,N-1
\end{aligned}
\tag{23}
$$

where $\Delta[\ ]$ denotes the difference of the bracketed function between $z^{(p)}+0$ and $z^{(p)}-0$. The nondiagonal terms in the right side of equation (23) represent the influence of the singularities of adjacent plies. These terms will become small if the subdivision of the p and p+1 is dense, since the nondiagonal terms contain the difference between the asymptotic solution and its polynomial approximation away from the singularity. However, for coarse subdivisions the contribution of the adjacent plies is significant for convergence.

8. SPLINE APPROXIMATION OF DISPLACEMENT COMPONENTS

The x, y and z displacement components are approximated by using cubic spline functions in curvilinear coordinates. The total displacement is approximated as:

$$u_i = \mathbf{C}_i \mathbf{X} \mathbf{U}_i^T + \delta_{i1} u_o \mathbf{X} \mathbf{E}^T, \tag{24}$$

where $\mathbf{X}$ is a vector of three-dimensional spline approximation basis functions, and $\mathbf{U}_i$ are the unknown spline approximation coefficients. The nonsquare matrices $\mathbf{C}_i$ and constant vector $\mathbf{E}$ are defined so that the approximation (24) is kinematically admissible, i.e. it satisfies boundary conditions (1) for arbitrary coefficients $\mathbf{U}_i$. Bold type will be used to distinguish vectors and matrices; superscript ^{T} means the transpose operation.

A detailed description of the spline approximation procedure and the properties of spline functions are given by Iarve [3]. The three-dimensional spline approximation functions are defined in curvilinear coordinates. The x,y plane was mapped into a region defined by ρ, ϕ, where $0 \le \rho \le 1$ and $0 \le \phi \le 2\pi$. The transformation was defined as follows:

$$x = \frac{D}{2} F_1(\rho) \cos\phi + L \cdot F_2(\rho)\alpha(\phi) + x_c$$
$$y = \frac{D}{2} F_1(\rho) \sin\phi + A \cdot F_2(\rho)\beta(\phi) + y_c \tag{25}$$

Functions F_1 and F_2 were defined as

$$F_1(\rho) = \begin{cases} 1 + \kappa \cdot \rho, \rho \le \rho_h \\ \dfrac{(1 + \kappa \cdot \rho_h)(1 - \rho)}{1 - \rho_h}, \rho_h \le \rho \le 1 \end{cases} \qquad F_2(\rho) = \begin{cases} 0, \rho \le \rho_h \\ \dfrac{\rho - \rho_h}{1 - \rho_h}, \rho_h \le \rho \le 1 \end{cases}$$

Coordinate line $\rho=0$ describes the contour of the hole, and the coordinate line $\rho=1$ describes the rectangular contour of the plate. Parameter κ defines the size of a near-hole region $D/2 \le r \le (1+\kappa)D/2$, which corresponds to $0 \le \rho \le \rho_h$, where a simple relationship between the polar coordinates and the curvilinear coordinates ρ, ϕ exists:

$$r - \frac{D}{2} = \frac{D\kappa}{2}\rho \quad \text{and} \quad \theta = \phi. \tag{26}$$

The width of this region is typically one hole radius, i.e., $\kappa\rho_h = 1$. Beyond this region a

transition between the circular contour of the opening and the rectangular contour of the plate

is performed. Functions $\alpha(\phi)$ and $\beta(\phi)$ describing the rectangular contour of the plate

boundary were given by Iarve *[3]*. These functions are introduced so that parametric

equations $x = \alpha(\phi) + x_c$, $y = \beta(\phi) + y_c$ describe the rectangular contour of the plate, and $0 \le \phi < \phi^{(1)}$

corresponds to $0 < x \le L, y = A$; $\phi^{(1)} \le \phi < \phi^{(2)}$ corresponds to $x = 0$, $0 < y \le A$; $\phi^{(2)} \le \phi < \phi^{(3)}$

corresponds to $0 \le x < L$, $y = 0$; and $\phi^{(3)} \le \phi < 2\pi$ corresponds to $x = L$, $0 \le y < A$.

Sets of one-dimensional cubic spline functions were defined in each coordinate

direction. Subdivisions were introduced through-the-thickness of each ply such that the p-th

ply, which occupies a region $z^{(p)} \le z \le z^{(p-1)}$, is subdivided into n_p sublayers. A set of

$N_z = \sum\limits_{p=1}^{N} n_p + 2N + 1$ basic B-type cubic spline functions $\{Z_i(z)\}_{i=1}^{N_z}$ with variable defect was

built along the z-coordinate according to a recurrent procedure given by Iarve *[3]*. These

cubic splines are twice continuously differentiable at all nodal points inside each ply and have

discontinuous first derivatives (the function itself is continuous) at the ply interfaces to

account for interfacial strain discontinuities. This is a necessary condition for traction

continuity at the ply interfaces. Nodal points are also introduced in the ρ and ϕ directions as

follows: $0 = \rho_0 < \rho_1 < .... < \rho_m = 1$, $0 = \phi_0 < \phi_1 < .... < \phi_k = 2\pi$. The subdivision of the ρ

coordinate is nonuniform. The interval size increases in geometric progression beginning at

the hole edge. The region $0 \le \rho \le \rho_h$ in which the curvilinear transformation is cylindrical is

subdivided into m_1 intervals ($m_1 < m$), so that $\rho_h = \rho_{m_1}$. Sets of basic cubic spline functions

$\left\{R_i(\rho)\right\}_{i=1}^{m+3}$, $\left\{\Phi_i(\phi)\right\}_{i=1}^{k+3}$ along each coordinate are built so that twice continuous derivatives in each node are provided. Splines along the ϕ are periodic at the ends of the interval. The vector of the three-dimensional spline approximation functions was defined as the tensor product of three one-dimensional sets of splines:

$$\left\{\mathbf{X}\right\}_q = R_i(\rho)\Phi_j(\phi)Z_l(z),$$
$$q = l + (j-1)N_z + (i-1)N_z k, \quad l = 1,...,N_z, j = 1,...,k, i = 1,...,m+3.$$

The components of vector $\mathbf{E}$ are equal to 1 or -1 for a component of $\mathbf{X}$ that is nonzero at $\rho=1$, $\phi^{(1)} \leq \phi < \phi^{(2)}$ ($x=0$) and $\rho=1$, $\phi^{(3)} \leq \phi < 2\pi$ ($x=L$), respectively. All other components of the vector $\mathbf{E}$ are equal to zero. The boundary matrices are obtained by deleting a number of rows from the unit matrix. The deleted rows have nonzero scalar product with $\mathbf{E}$.

The region Γ of the hybrid approximation superposition is inside the region in which the transformation (25) coincides with (26). The boundary $r=r_0$ is defined to coincide with the radial coordinate line so that $r_0 = \dfrac{D}{2}(1 + \kappa\rho_{m_0})$, where $m_0 \leq m_1$. A reduced set of splines in the ρ –direction $\left\{R_i^s(\rho)\right\}_{i=1}^{m_h+3}$ is defined only over the first m_1 intervals for the purpose of efficient solution of the systems of equations for determining $u_i^{s,p}$. It is built exactly the same way as the one over the entire interval. It can be shown that the reduced set is a subset of the approximation (24).

The approximation of the singular displacements can be written as

$$u_i^{s,p} = \mathbf{C}_i^p \mathbf{X}^s \mathbf{U}_i^{p^T} \tag{27}$$

where $\mathbf{U}_i^p(\theta)$ are unknown coefficients and

$$\{\mathbf{X}^s\}_q = R_i^S(\rho)Z_l(z),$$

$$q = l + (i-1)N_z,$$

$$l = 1,...,N_z, \, j = 1,...,k, \, i = 1,...,m_1 + 3.$$

Matrices $\mathbf{C}_i^p$ are defined to satisfy boundary conditions (20). The truncated in-plane derivatives in equation (19) are calculated as:

$$\left(\frac{\partial}{\partial x}\right)_\theta = \frac{2}{D\kappa}\cos\phi\frac{\partial}{\partial\rho}, \quad \left(\frac{\partial}{\partial y}\right)_\theta = \frac{2}{D\kappa}\sin\phi\frac{\partial}{\partial\rho},$$

9. NUMERICAL RESULTS

9.1 Uniaxial Tension of [45/90/-45/0]$_s$ Laminate

A [45/90/-45/0]$_s$ quasi–isotropic IM7/5250-2 laminate was considered, where the stacking order is from the top to the central plane, reading from left to right, respectively. The elastic properties of the unidirectional ply were E_1 =151 GPa, $E_2=E_3$=9.45 GPa, $G_{12}=G_{13}$=5.9 GPa, G_{23}=3.26 GPa, $v_{12}=v_{13}$=0.32, and v_{23}=0.45. The in-plane dimensions of the plate were L=290 mm, A=76 mm, x_c=L/2, y_c=A/2, D=12.5 mm and the ply thickness h=1.34 mm.

The average applied stress was calculated as

$$\sigma_0 = \frac{1}{AH} \int_0^A \int_o^H \sigma_{xx}(L, y, z) dy dz \qquad (28)$$

Figure 2 shows the power of singularity calculated for each interface as a function of the polar angle; it varies for stresses from –0.01 to –0.077 depending on the angle. Two mesh densities were used for obtaining the coefficient of the singular term under the uniaxial loading boundary conditions (1). Coarse subdivision was defined as follows.

   z-coordinate: 1 sublayer per ply

   ρ-coordinate: m=12, m_0=8, κp_h = 1, q=1.2.

   θ-coordinate: 48 equal intervals.

The fine subdivision consisted of:

   z-coordinate: 3 nonuniform (1:2:1) sublayers per ply

   ρ-coordinate: m=24, m_0=20, κp_h = 1, q=1.2.

   θ-coordinate: 48 equal intervals.
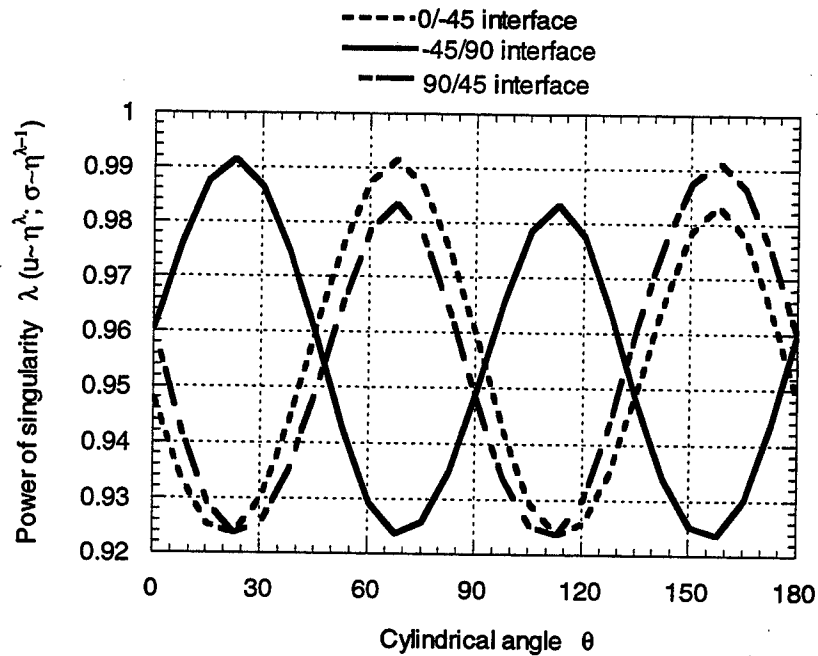
Figure 2. **Power of Singularity versus Cylindrical Angle at all Interfaces of the [45/90/-45/0]ₛ Laminate.**

The coefficient of the singular stress term calculated by using these subdivisions is shown in Figure 3 at each interface. The values obtained by using equation (23) and the values calculated by retaining only the diagonal terms on the right-hand side of equation (23) are compared. For the coarse subdivision the nondiagonal terms are very significant, so that the values obtained by neglecting them may even be of different sign. For the fine subdivision the two results are almost identical. Indeed, the magnitudes of the nondiagonal terms are determined by the accuracy of approximation of the singular stress term by the polynomial approximation one or more ply thicknesses away from the singularity. The density of the subdivision through the ply thickness defines this accuracy. The values of the K_4, K_5 and K_6 obtained with the two subdivisions and taking into account the nondiagonal terms are close together. Figure 4 shows the characteristics of the singular behavior of the interlaminar shear stresses, namely:

26

(a)

(b)

(c)
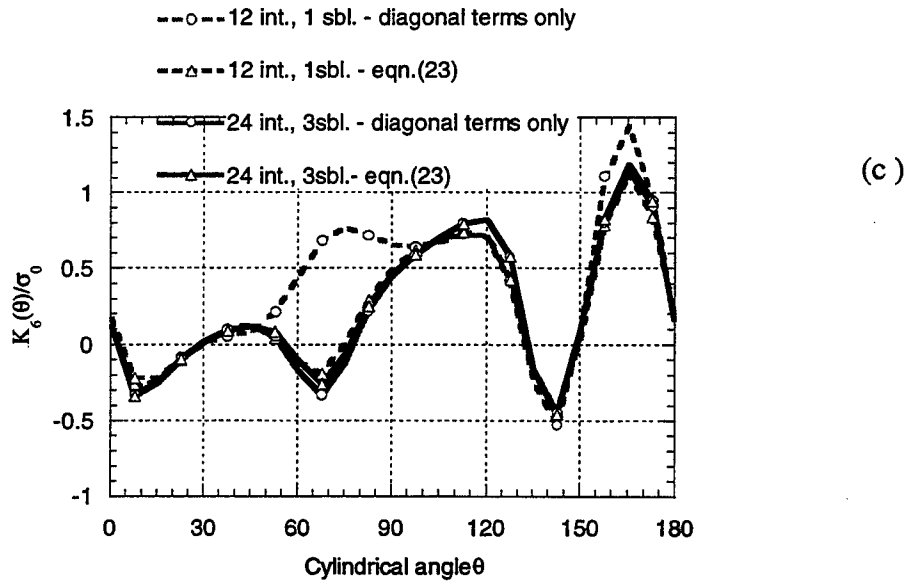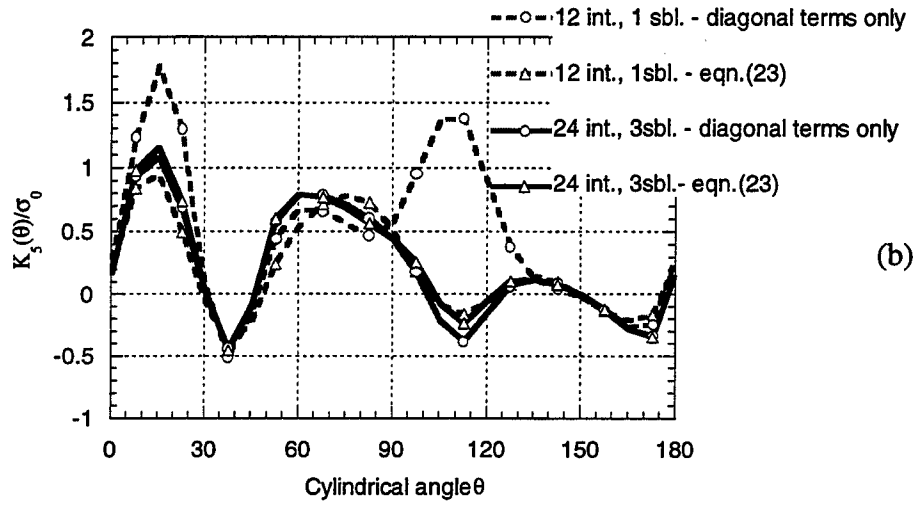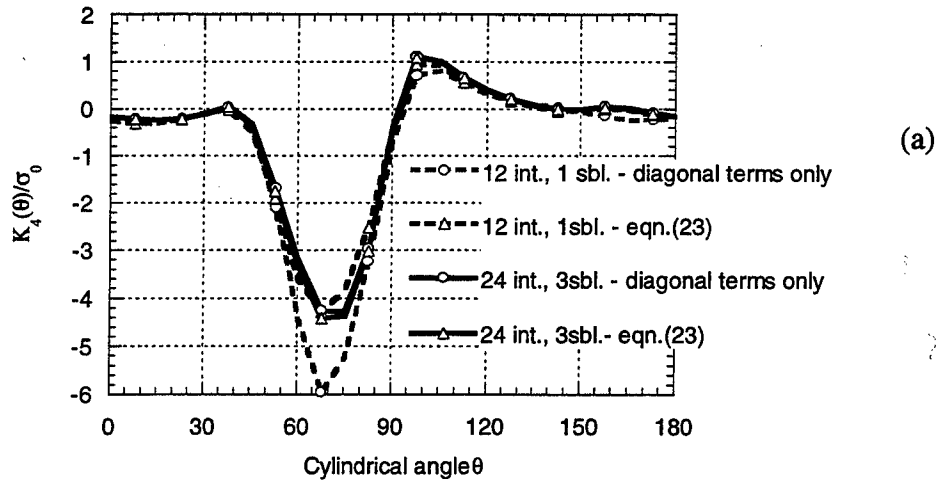
Figure 3. Singular Term Coefficients at Different Interfaces for the [45/90/-45/0]ₛ Laminate under Uniaxial Loading.
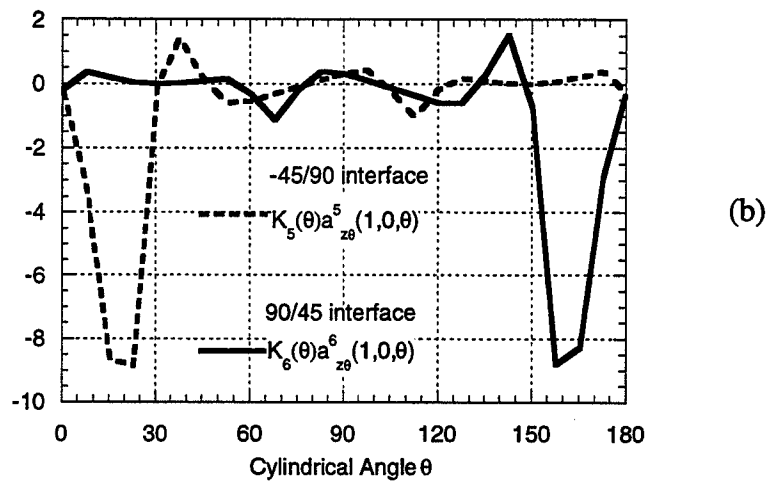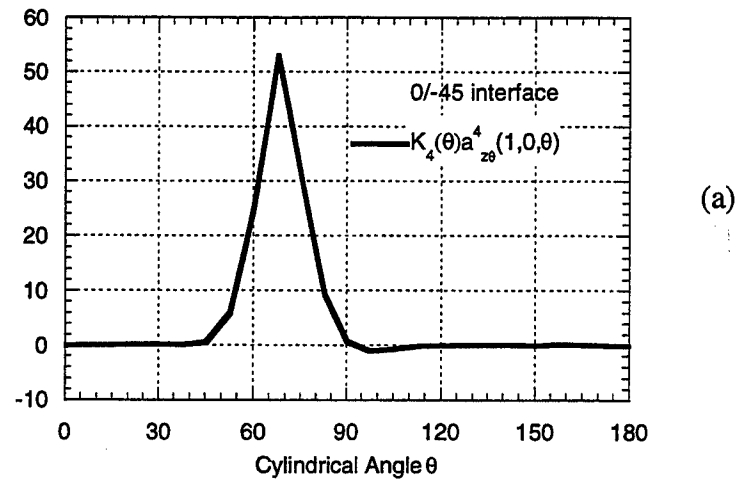
(a)

(b)

(c)
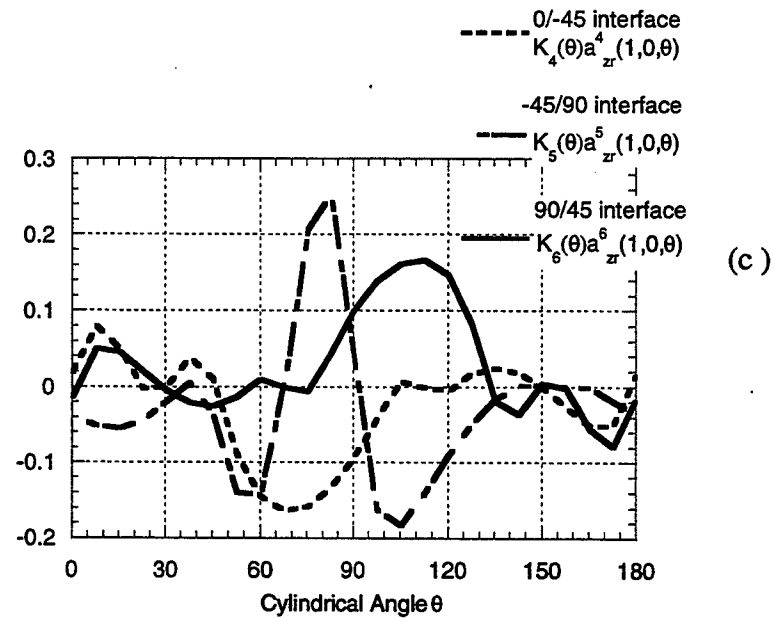
Figure 4. **Transverse Shear Stress Normalized Singular Term Coefficients at Different Interfaces for the [45/90/-45/0]$_s$ Laminate under Uniaxial Loading.**

28

$$\lim_{\eta \to 0} \eta^{1-\lambda} \sigma_{z\theta}(D/2+\eta, z^{(p)}, \theta) = K_p a_{z\theta}^p(1,0,\theta)$$

$$\lim_{\eta \to 0} \eta^{1-\lambda} \sigma_{zr}(D/2+\eta, z^{(p)}, \theta) = K_p a_{zr}^p(1,0,\theta) \quad ,$$

where K_p were determined by the fine mesh solution.

Interlaminar stress components at a $\theta=60.3^0$ cross section, normalized by the average applied stress (28), will be considered in Figures 5-8. The transverse radial shear component on all interfaces calculated by using the fine subdivision is shown in Figure 5. Stresses σ_{rz}^u are displayed in Figure 5a. At the 0/-45 and -45/90 interfaces, we observe the typical discontinuity of σ_{rz}^u, near the singularity, whereas the interface 90/45 shows relatively continuous traction up to the singular point. This is in agreement with Figure 4c, showing very small amplitude of the singular term at the latter interface compared to the two others at $\theta=60.3^0$. The stresses calculated according to hybrid approximation (21) are shown in Figure 5b. It should be noted that the closest point to the singularity shown in this figure is r=D/2+0.002H. The traction discontinuity is practically indistinguishable within the graphic resolution.

The transverse normal stresses are examined in Figures 6 and 7. The σ_{zz}^u stresses on all three interfaces are shown in Figures 6a and 6b. The difference between the results obtained with two subdivisions is clearly observed for (r-D/2)/H<0.6. The values obtained by using the hybrid approximation are displayed in Figure 7. In this case the two subdivisions give practically identical results. We observe (Figure 8) a small absolute value of K (60.3^0) at the 90/45 interface. This led to an inconclusive σ_{zz} trend definition based on equation (17) as shown in Figure 6a. The hybrid approximation in Figure 7a shows that this interface is in
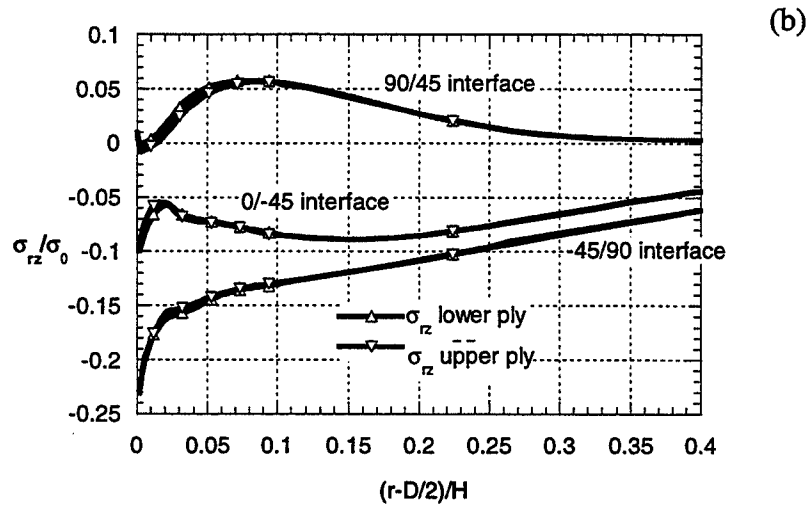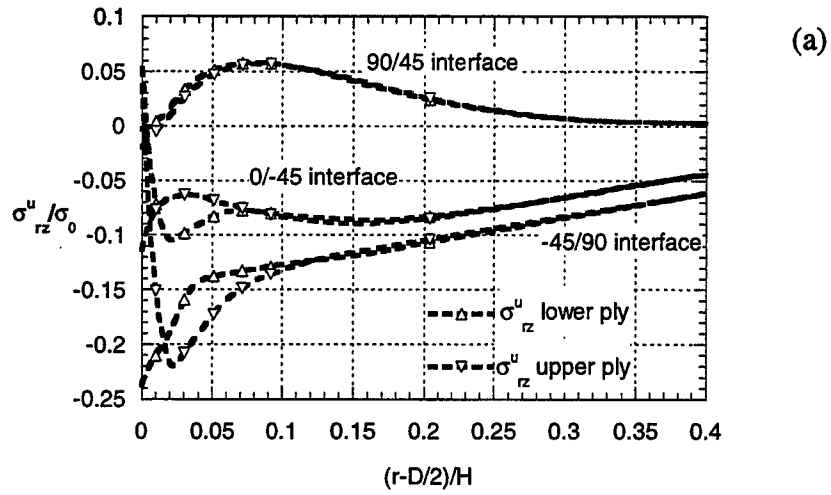
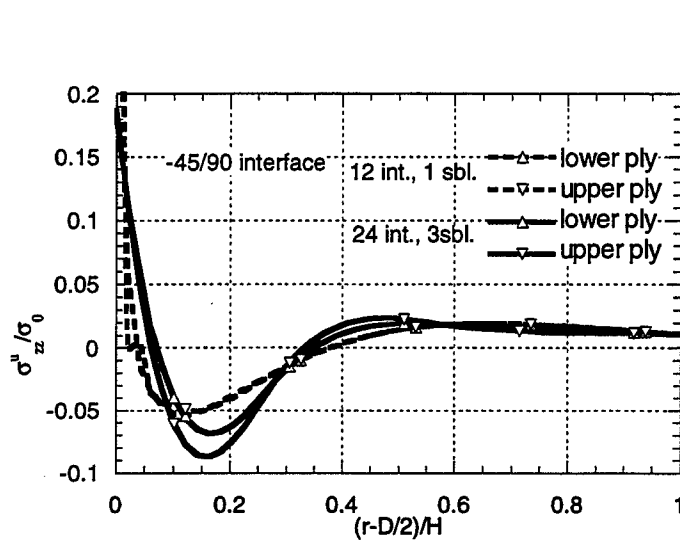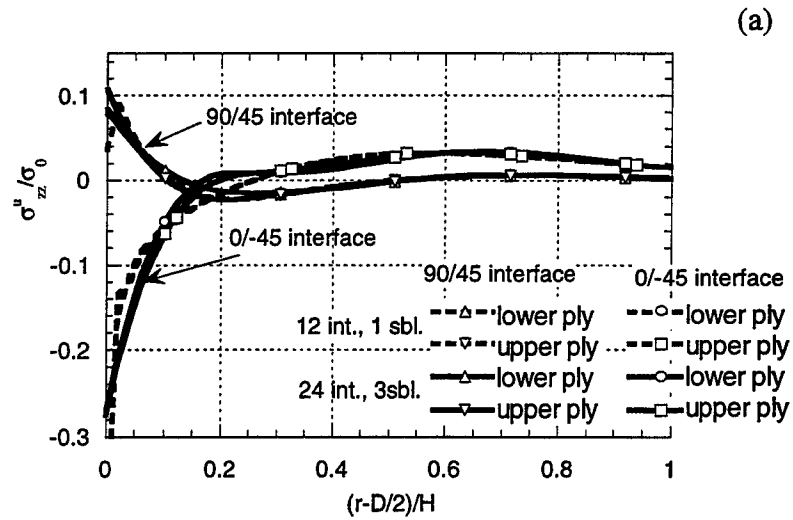**Figure 5. Transverse Interlaminar Shear Stress at θ=60.3°.**

Figure 6. Transverse Interlaminar Normal Stress at $\theta=60.3°$ Obtained by Using Displacement Approximation.
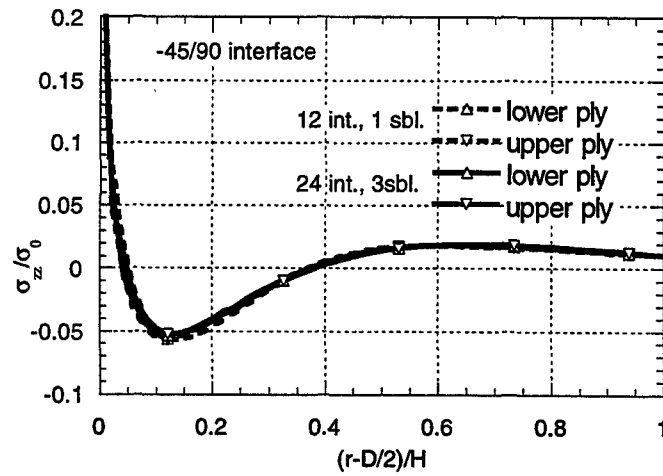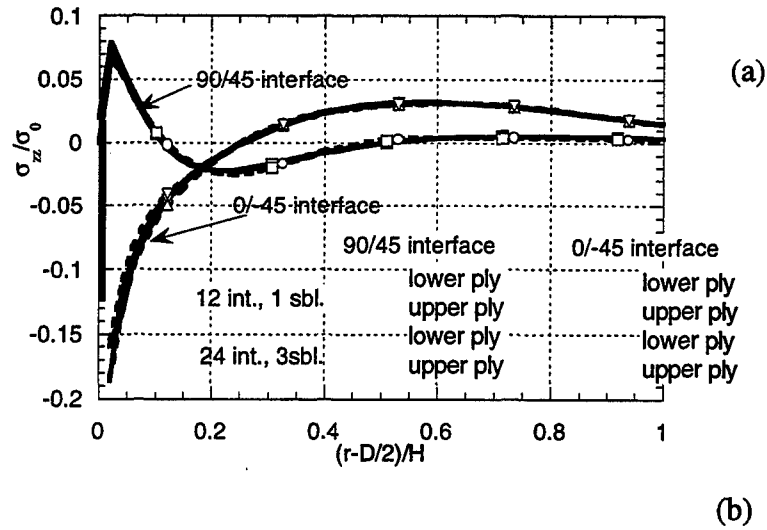
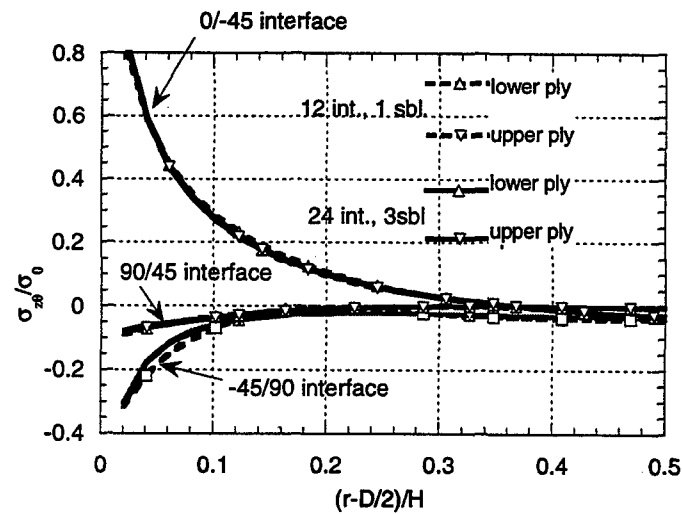Figure 7. Transverse Interlaminar Normal Stress at θ=60.3° Obtained by Using Hybrid Approximation.

Figure 8. Transverse Interlaminar Shear Stress at θ=60.3°.

compression along with the 0/-45 interface. The -45/90 interface exhibits a tensile peel stress singularity, which is in agreement with Figure 8.

The $\sigma_{z\theta}$ obtained by using the hybrid approximation with the two subdivisions are shown in Figure 8 for completeness. The fine and the coarse subdivision provide very close agreement in the stress values which is indicative of convergence.

9.2   Thermal Stresses in a [45/90/-45/0]$_s$ Laminate

The same laminate is considered under a uniform temperature change of $\Delta T = -167^0C$. This temperature drop is used to approximate the residual stresses generated during the processing cool-down phase. The displacement boundary conditions (1) are modified so that the edge x=L is released (zero tractions). The coefficients K_4, K_5 and K_6 obtained with the coarse and fine subdivisions described in the previous section are shown in Figure 9. Some differences between the coarse and fine mesh analysis results can be seen for low values, while all the maximum values are practically identical. The values of the coefficients are positive at all interfaces in all circumferential directions. Therefore, a tensile peel stress is expected near singularities. Figure 10a shows the transverse normal stresses σ_{zz}^u obtained with the coarse subdivision based on displacement approximation in the cross section $\theta=157.8^0$, where the maximum value of K occurs. The stresses are displayed at two interfaces in the top (solid line) and bottom (dashed line) plies. The normal stresses are seemingly discontinuous a distance of approximately 0.6H from the hole edge. Figure 10b shows the same stresses at all interfaces calculated using the hybrid approximation (21). The
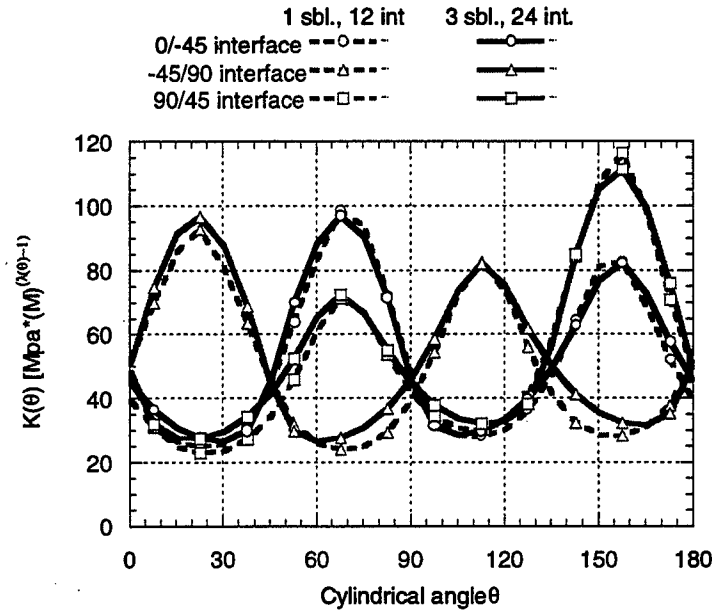
Figure 9. **Singular Term Coefficients at Different Interfaces for the [45/90/-45/0]$_s$ Laminate under Thermal Loading.**

while all the maximum values are practically identical. The values of the coefficients are positive at all interfaces in all circumferential directions. Therefore, a tensile peel stress is expected near singularities. Figure 10a shows the transverse normal stresses σ_{zz}^u obtained with the coarse subdivision based on displacement approximation in the cross section $\theta=157.8°$, where the maximum value of K occurs. The stresses are displayed at two interfaces in the top (solid line) and bottom (dashed line) plies. The normal stresses are seemingly discontinuous a distance of approximately 0.6H from the hole edge. Figure 10b shows the same stresses at all interfaces calculated using the hybrid approximation (21). The discontinuities are reduced significantly. It is interesting to point out that the σ_{zz}^u stress at the 90/45 interface obtained with coarse subdivision in Figure 10a may appear to have a tendency towards $-\infty$ as one approaches the interface. The hybrid approximation shows a
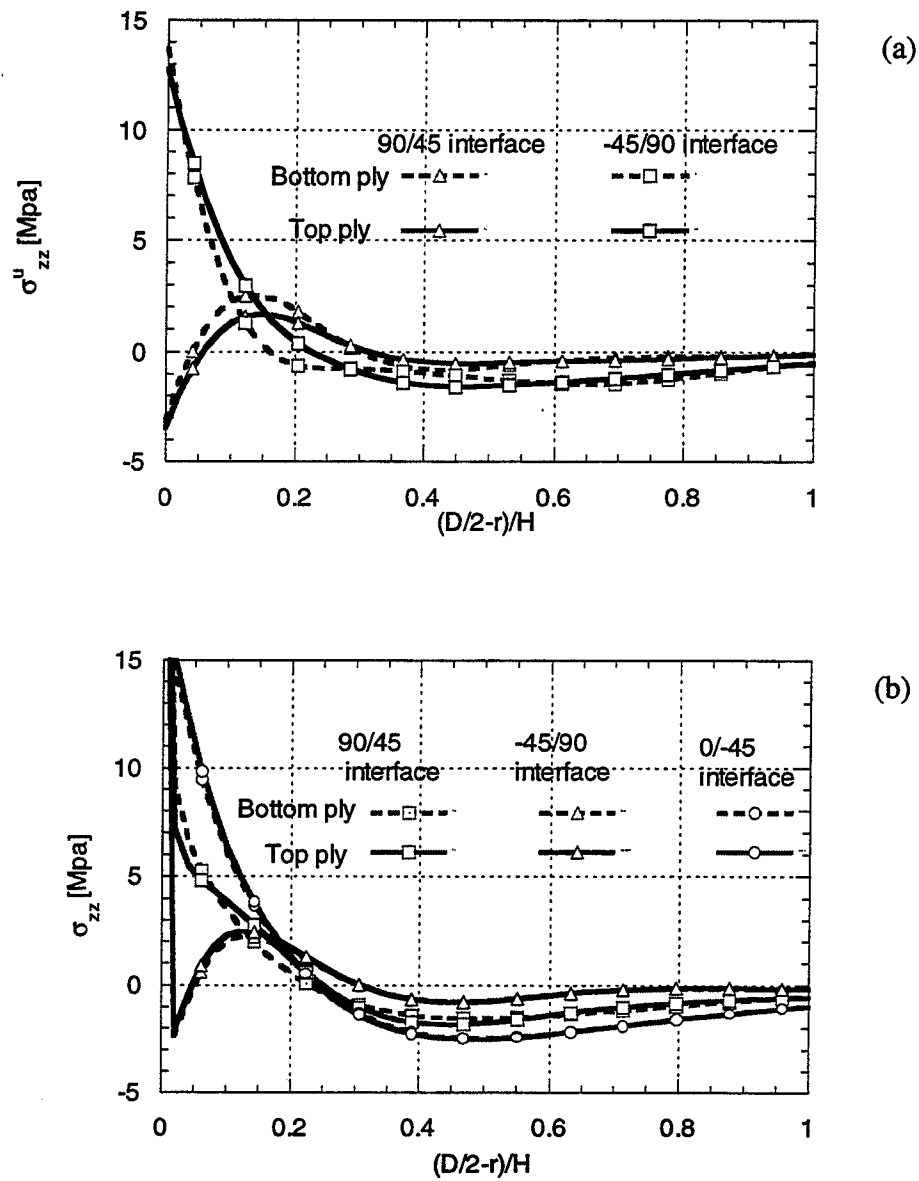
34

Figure 10. Transverse Interlaminar Normal Stress at θ=157.3° Obtained by Using Displacement Approximation with Coarse Subdivision.

sharp change of sign very close to the singularity. This trend is picked up by the approximation using fine subdivision as shown in Figure 11a. In this case the tractions at the bottom and top surfaces are continuous starting from 0.2H from the hole edge. The hybrid approximation (Figure 11b) provides traction values with imperceptible discontinuities everywhere. The hybrid stresses obtained with the two subdivisions, Figures 10b and 11b, are practically the same.

9.3   Bearing Loading of a [45/-45]$_s$ Laminate

A square [45/-45]$_s$ plate is considered. The geometric properties are L=A=508 mm, D=50.8 mm, ply thickness h=5.1 mm, E_1=138 GPa, E_2=E_3=14.5 GPa, G_{12}=G_{13}=G_{23}=5.9 GPa and v_{12}=v_{13}=v_{23}=0.21. The displacement boundary conditions were applied so that u_0/L=0.001. The average applied stress σ_0 was calculated afterwards according to equation (28) and used to normalize the results. Formulation and solution of the three-dimensional contact interaction problem based on B-spline displacement approximation is given in reference [5]. Two subdivisions were used for the convergence study. The θ coordinate in all cases was uniformly divided into 48 intervals. The "coarse" subdivision consisted of n_s=1-one sublayer per ply in the z-direction, and a total of m=12 nonuniform intervals for the ρ coordinate. The consecutive interval length ratio was q=1.2 starting from the hole edge. The "fine" subdivision contained n_s=4 sublayers per ply thickness and ρ coordinate: m=24, q=1.4.

Asymptotic analysis revealed that a real, near-singular, root $1 \leq \lambda < 1.15$ is present at the filled-hole edge in this problem. The singular ($0 < \lambda < 1$) and the near singular, root $1 \leq \lambda < 1.15$ are shown in Figure 12. The singular root of the open-hole solution is also shown
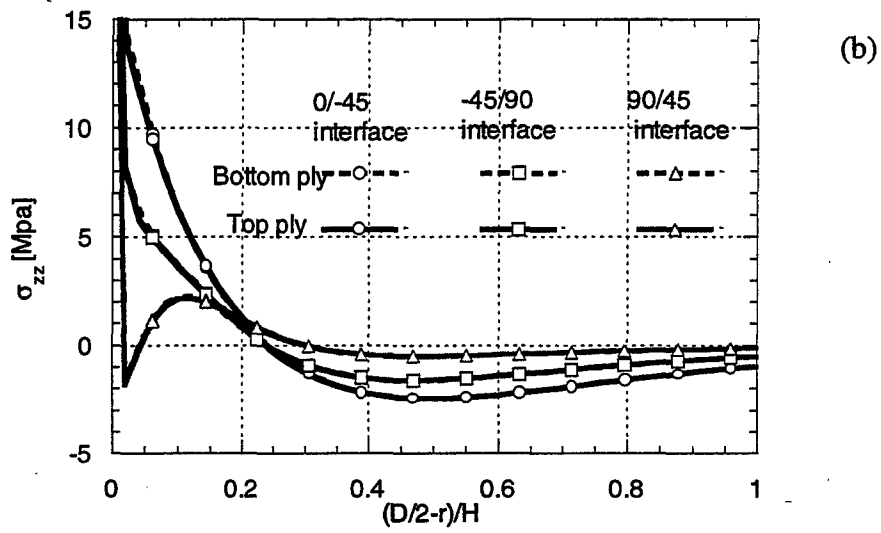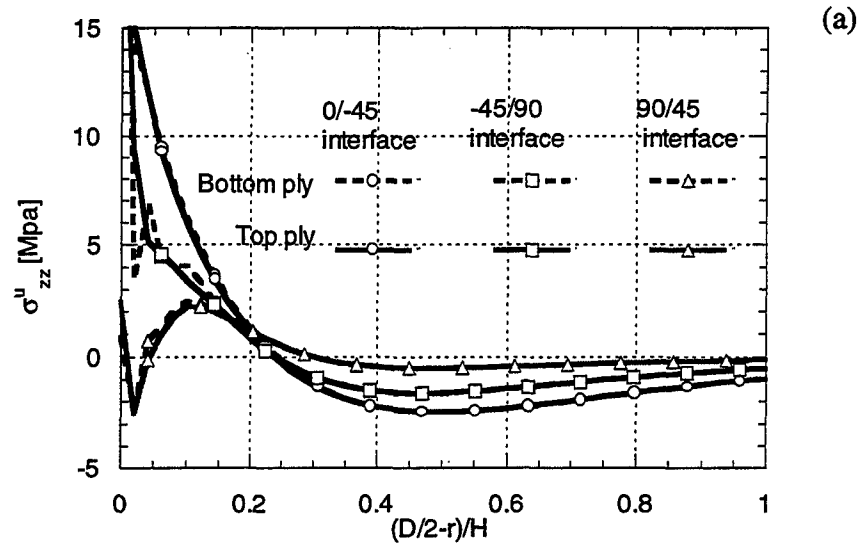
Figure 11. Transverse Interlaminar Normal Stress at θ=157.3° with Fine Subdivision.
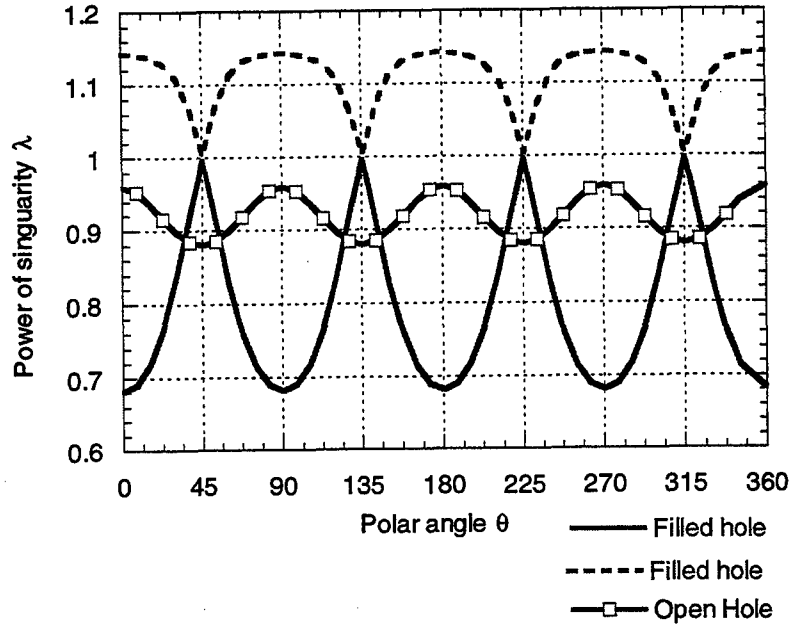
Figure 12. **Roots of the Asymptotic Solution for Stress Distributions near the Filled- and Open-Hole Edge Singularity for [45/-45] Interface.**

for comparison. It must be noted that $\lambda=1$ is also a root; however, the stress field which it creates is constant and therefore its spline approximation projection will be exactly equal to it, i.e. $a_{ij}^2 - s_{ij}^2 \equiv 0$. It was found that at locations $\theta=45, 135, 225, 315$, the singular root becomes equal to unity as well as the near-singular root. At these locations the singularity disappears, and, according to the fact that $a_{ij}^m - s_{ij}^m \equiv 0, m = 1,2,3$, an instability of determination of K_m is expected. Two roots, $\lambda_1 \leq 1$ and $1 \leq \lambda_3 < 1.15$, were included into approximation (15) at each circumferential location $93 < \theta < 267$ which corresponds to the contact zone.

Collocation points were ρ_0 and ρ_1. The multiplicative term K_1 as a function of θ obtained with the two subdivisions is shown in Figure 13. The dashed regions surround the $\theta=135$ and 225 locations where the root equality occurs. Outside these regions the results obtained with
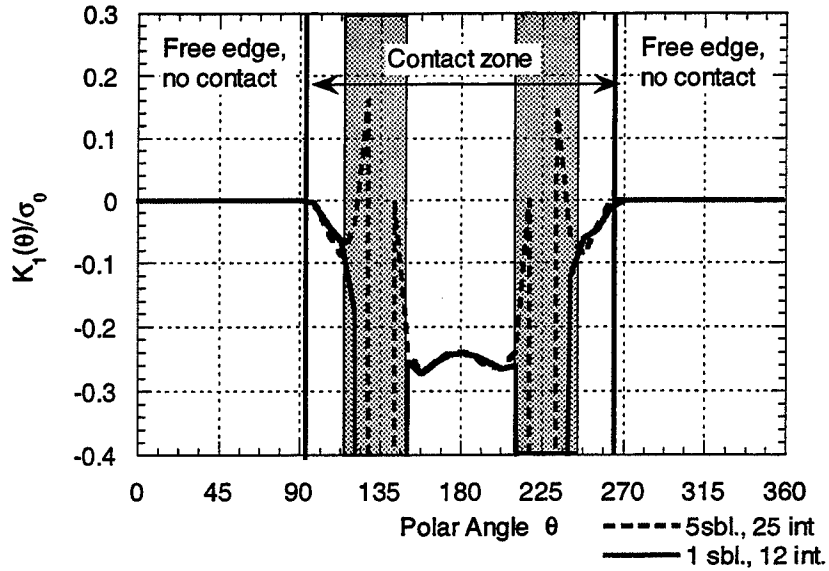
38

Figure 13. **Multiplicative Factor of the Singular Term of the Filled-Hole Asymptotic Solution in the Bearing Loading Problem for [45/-45]$_s$ Laminate.**

the two subdivisions are very close and indicate convergence. The interlaminar shear stress σ_{rz} component is shown in Figure 14 for $\theta=180$ on the interface $\psi=0$. Dashed lines show the stresses (16) at the interface calculated from displacements (7) directly using Hooke's law. The stress values in the upper and lower ply are discontinuous for both subdivisions. The region of discontinuity shrinks while increasing the subdivision, however, the amplitude of the discontinuity at the hole edge increases at the same time. A similar effect at the open-hole edge was explained due to directional nonuniqueness of the asymptotic behavior [2]. The hybrid approximation (15) provides traction continuity and converged stresses even for the coarse subdivision, as shown by solid lines. Chaotic behavior of the multiplicative factor K_1 near $\theta=135$ and 225 has been anticipated. However, the stress behavior at these locations
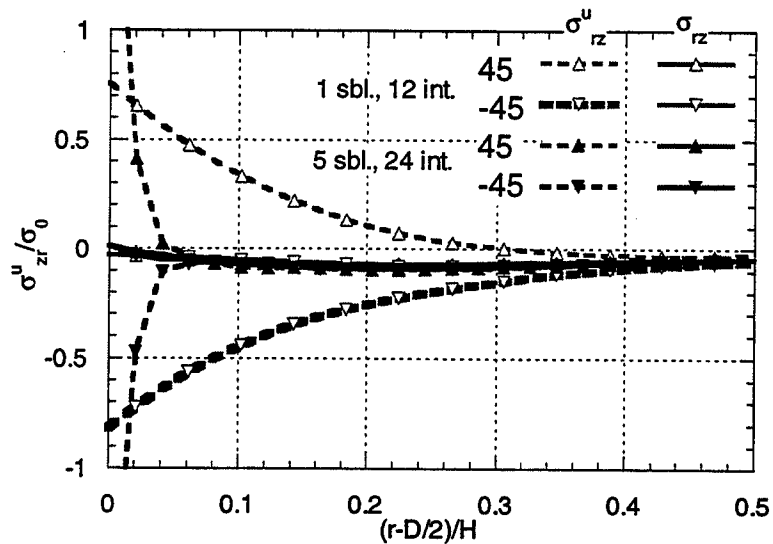
Figure 14. **Interlaminar Transverse Shear Stress in the θ=180° Cross Section in the Bearing Loading Problem for [45/-45]$_s$ Laminate.**

is expected to exhibit convergence since the singularity disappears. Figure 15 displays the same as the previous figure at θ=135. Only the stress values calculated from displacements (7) directly are shown. The traction discontinuity observed for the coarse subdivision is an order of magnitude lower than at θ=180. It can be also seen that the fine subdivision provides traction continuity at the hole edge, thus manifesting absence of the singularity. It should be noted that further development is required to describe the behavior of the multiplicative factor K_1 in the regions where the singularity impairs.
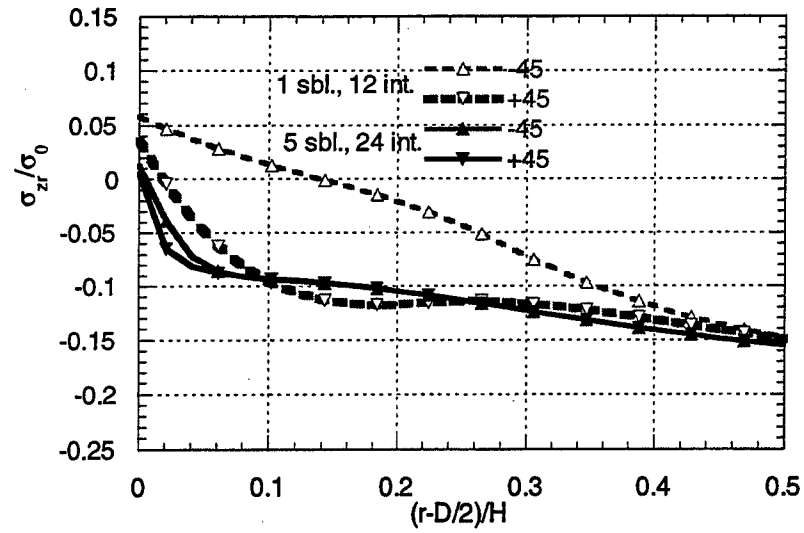
40

Figure 15. Interlaminar Transverse Shear Stress in the $\theta=135°$ Cross Section in the Bearing Loading Problem for $[45/-45]_s$ Laminate.

10. CONCLUSIONS

1. The method of superposition of hybrid and displacement approximations was extended to provide accurate stress fields in the vicinity of the ply interface and the hole in practical laminates with multiple interfaces. The asymptotic analysis was used to derive the hybrid stress functions. The displacement approximation was based on polynomial B-spline functions.

2. The coefficients of the singular terms in stress solution near the ply interfaces and the open-hole edge were determined in quasi-isotropic $[45/90/-45/0]_s$ laminates under mechanical and thermal loading. Convergence studies showed that accurate values of the coefficients of the singular terms can be obtained with the coarse out-of- plane subdivision of one sublayer per ply. It was shown that for laminates with multiple interfaces, the influence of singular terms on adjacent interfaces is important for coarse subdivision convergence.

3. Coefficients of the singular term of the asymptotic expansion were determined for $[45/-45]_s$ laminate under bearing loading introduced through a rigid fastener.

11. PUBLICATIONS AND PRESENTATIONS

The following is a list of presentations and publications that were generated during this contractual period.

Iarve, E. V. (1997, November). *3-D Asymptotic and B-Spline Approximation Analysis in Composite Laminates with Open and Filled Holes*. Presented at the ASME Winter Meeting, Dallas, TX.

Iarve, E. V. (1998). Three-Dimensional Stress Analysis in Open-Hole Composite Laminates Containing Matrix Cracks. *Proc. of AIAA SDM Conference.*

Iarve, E. V. (1998). Combined Asymptotic and B-Spline Based 3-D Analysis of Rigid Fastener Hole Composites. *Proc. ICCE/5* (p. 403).

Iarve, E. V. (1998, accepted). Singular Full-Field Stresses in Composite Laminates with Open Holes. *Int. J. Solids Structures.*

12. REFERENCES

1. Iarve, E. V. (1998). Spline Variational Theory for Composite Bolted Joints (AFRL-ML-TR-1998-4020). Dayton, OH: U.S. Air Force.

2. Iarve, E. V. (1997). Combined Asymptotic and B-Spline Based Approximation for 3-D Stress Analysis of Composite Laminates with Holes. *Proc. 38th AIAA SDM Conference.*

3. Iarve, E. V. (1996). Spline Variational Three-Dimensional Stress Analysis of Laminated Composite Plates with Open Holes. *Int. J. Solids Structures 44*(14) (2095-2118).

4. Wang, S. S., & X. Lu. (1993). Three-Dimensional Asymptotic Solutions for Interlaminar Stresses Around Cutouts in Fiber Composite Laminates. In Y. D. S. Rajapakse, ed., *Mechanics of Thick Composites* (AMD-Vol. 162, Book No. G00785, pp. 41-50).

5. Iarve, E. V. (1997). 3-D Stress Analysis in Laminated Composites with Fasteners Based on the B-Spline Approximation. *Composites Part A*, Vol.28A (559-571).

APPENDIX

$$A_{11} = Q_{11}^{(s)}\cos^2\theta + Q_{16}^{(s)}\sin2\theta + Q_{66}^{(s)}\sin^2\theta, \quad A_{12} = Q_{16}^{(s)}\cos^2\theta + \left(Q_{12}^{(s)}+Q_{66}^{(s)}\right)\sin\theta \cos\theta + Q_{62}^{(s)}\sin^2\theta,$$

$$A_{22} = Q_{66}^{(s)}\cos^2\theta + Q_{26}^{(s)}\sin2\theta + Q_{22}^{(s)}\sin^2\theta, \quad A_{33} = Q_{55}^{(s)}\cos^2\theta + Q_{54}^{(s)}\sin2\theta + Q_{44}^{(s)}\sin^2\theta,$$

$$A_{21} = A_{12}, \quad A_{31} = A_{13} = A_{32} = A_{23} = 0,$$

$$B_{31} = \left(Q_{13}^{(s)}+Q_{55}^{(s)}\right)\cos\theta + \left(Q_{63}^{(s)}+Q_{54}^{(s)}\right)\sin\theta, \quad B_{32} = \left(Q_{63}^{(s)}+Q_{45}^{(s)}\right)\cos\theta + \left(Q_{23}^{(s)}+Q_{44}^{(s)}\right)\sin\theta,$$

$$B_{21} = B_{12} = B_{11} = B_{22} = B_{33} = 0, \quad B_{13} = B_{31}, B_{23} = B_{32},$$

$$C_{11} = Q_{55}^{(s)}, \quad C_{12} = Q_{54}^{(s)}, \quad C_{22} = Q_{44}^{(s)}, \quad C_{33} = Q_{33}^{(s)},$$

$$C_{21} = C_{12}, \quad C_{31} = C_{11} = C_{32} = C_{23} = 0.$$

Ply stiffness coefficients $Q_{ij}^{(s)}$ s=1,..,N are contracted notations of the fourth-order tensor $C_{ijkl}^{(s)}$, used in the text.